INSTITUTE OF PHYSICS PUBLISHING JOURNAL OF OPTICS B: QUANTUM AND SEMICLASSICAL OPTICS
J. Opt. B: Quantum Semiclass. Opt. **6** (2004) S430–S435 PII: S1464-4266(04)71455-X

Mechanisms of crossing for an X-junction based on dark spatial solitons*

M Torres-Cisneros[1], L A Aguilera-Cortés[1], M A Meneses-Nava[2], J J Sánchez-Mondragón[3,4] and G E Torres-Cisneros[5]

[1] FIMEE, Universidad de Guanajuato, Salamanca, Guanajuato México, Mexico
[2] Optical Properties of the Matter, CIO, León, Gto. México, Mexico
[3] Photonics and Optical Physics, INAOE, Puebla, Puebla México, Mexico
[4] CIICAp, UAEM, Cuernavaca, Morelos México, Mexico

Received 31 October 2003, accepted for publication 6 January 2004
Published 4 May 2004
Online at stacks.iop.org/JOptB/6/S430
DOI: 10.1088/1464-4266/6/5/034

Abstract
We present a fundamental study on the capability of a crossing of two optical waveguides based on dark spatial solitons to act as a controllable optical beam splitter. Our study is based on the fact that the guided beam is diffracted at the waveguide crossing by an effective phase screen formed by the soliton collision profile. We find that when the two dark solitons are immersed into the same finite bright background, the energy of a guided beam can be split into the desired optical channel according to the collision angle. We also found that even the corresponding phase diffractive screen possesses a quite different structure in the bright and dark soliton cases; the physics involved is the same.

Keywords: dark spatial solitons, nonlinear materials, logic gates, X-couplers

1. Introduction

Controlling light-by-light represents the aim of photonics, and spatial solitons seem to be good candidates to accomplish some of the required operations and functions. The control of spatial solitons can be carried out, for example, by the presence of another soliton through the inherent forces between them. Optical logic gates based on the changes of position that take place during a bright-spatial soliton collision (Islam *et al* 1992), or during the interaction of two close solitons (Kodama and Hasegawa 1991) can be constructed.

In this way, spatial solitons can also control the trajectory of weak beams if they are used as optical waveguides. Two fundamental ways of doing so with bright spatial solitons have been proposed. In the first approach, a weak beam guided by one spatial soliton follows the resulting trajectory when the soliton interacts with another close soliton (Shalaby and Barthelemy 1992). In the second case, the trajectory of the weak beam is controlled by an effective grating phase diffraction when the soliton collides with another soliton (Luther-Davies and Xiaoping 1992). On the other hand, controlling weak beams is also possible in a self-defocusing medium, and a good example is the optical Y junction obtained when a weak beam is forced to follow the optical waveguides emerging from a secondary dark spatial soliton generation (Zhao and Bourkoff 1989). However, to the best of our knowledge, no attempts have made to explore the possibilities of controlling weak beams making use of dark spatial soliton interaction or collision.

The interaction between two ideal dark solitons is governed by an effective repulsive force in contrast with the force between two bright solitons, which depends on the relative phase of the solitons (Tomlinson and Hawkings 1989).

Ideal dark spatial solitons require finite transversal intensity as $x \rightarrow \pm\infty$. Instead, a real dark spatial soliton consist of an intensity depletion into a finite bright background. Numerical results have demonstrated that a real dark spatial soliton exhibits quasi soliton behaviour provided the width of the bright background is at least ten times the width of the soliton (De la Fuente *et al* 1991). A similar conclusion applies for the collision of two real dark solitons if they are immersed into the same bright background (Thurston and Weiner 1991). However, if the spatial solitons are used as optical waveguides,

* The authors would like to dedicate this work to the memory of G E Torres-Cisneros.
[5] In memoriam.

a practical situation is that each dark soliton possesses its own finite bright background beam. Nevertheless, this bright background beam will become chirped because of the simultaneous effects of diffraction and self-defocusing (Thurston and Weiner 1991), and it is expected that this will affect the dynamics of a quasi-dark soliton of a collision of two optical channels (Torres-Cisneros *et al* 1995).

In this paper we analyse the physical properties of a collision of two optical waveguides based on ideal dark spatial solitons, in order to explain the physical mechanisms which can operate in an X-junction. We know the essential differences between bright and dark soliton behaviour, nevertheless, through this work we will use some useful analogies. In section 2 we provide the theoretical model and some numerical solutions for the real dark spatial soliton. The characterization of an X-junction based on the collision of two ideal dark spatial solitons is analysed in section 3. Finally, section 4 gives the conclusions of our work.

2. Theory

We are interested in describing the behaviour of a guided beam during a crossing of two optical waveguides based on ideal dark spatial solitons. Physically, this situation is met for example, when the two dark solitons are immersed into the same sufficiently wide bright background. The appropriate physical model is given by the coupling of two laser beams with the same polarization, but with different wavelength, within a negative Kerr-type medium (De la Fuente *et al* 1991). We assume that the beams propagate in the positive direction of the Z-axes, and that the physical conditions for a two-dimensional approach are satisfied. From the mathematical point of view, the waveguide property of a spatial soliton is explained in terms of the cross-phase modulation effect in a Kerr medium (Agrawal 2002). Denoting by A_1 and A_2 the normalized transversal envelopes of the strong and weak beams, respectively, their evolutions within the nonlinear medium are governed by

$$\mathrm{i}\frac{\partial A_1}{\partial Z} = \frac{1}{2}\frac{\partial^2 A_1}{\partial X^2} - |A_1|^2 A_1 - 2|A_2|^2 A_1 \tag{1}$$

$$\mathrm{i}\frac{\partial A_2}{\partial Z} = \frac{1}{2} r_n \frac{\partial^2 A_2}{\partial X^2} - 2\beta|A_2|^2 A_2 - \beta|A_1|^2 A_2 \tag{2}$$

where the linear approximation ($|A_1|^2 \gg |A_2|^2$) could neglect the terms with $|A_2|^2$. In equations (1) and (2) the propagation distance Z is measured in units of the diffraction length of the intense beam, while the transversal distance X is normalized to the initial width of the intense beam. In equation (2) $r_n = n_{01}\lambda_2/n_{02}\lambda_1$, with n_{0i} is the linear refractive index of the medium at wavelength λ_i, and $\beta = 2\lambda_1/\lambda_2$.

Because equation (1) is the NLSE it admits single and multiple dark soliton solutions (Blow and Doran 1985), and among them we take for this section that which describes the collision of two dark solitons. For the specific case of two dark solitons of the same amplitude, travelling with opposite transversal velocities, the two dark soliton solution takes the form (see equation (10) of Blow and Doran (1985)):

$$A_1(x, z) = 1 - \frac{2\mathrm{i} f(x, z)}{g(x, z)} \tag{3}$$

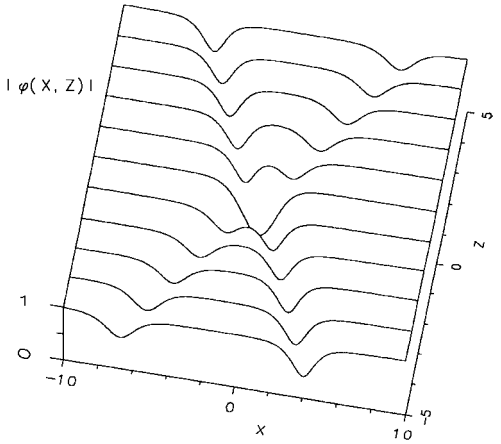

Figure 1. Crossing of two optical waveguides based on dark solitons as they propagate within the nonlinear medium. The graph was obtained evaluating equation (2) at the indicated propagation distances Z, with $\varsigma_1 = 0.6$ and $\varsigma_2 = -0.4$.

where

$$f(x, z) = \frac{2}{\mu_1 + \mu_1}\left(\frac{1}{\varsigma_1 + \mathrm{i}\mu_1} + \frac{1}{\varsigma_2 + \mathrm{i}\mu_2}\right) - (\varsigma_1 + \mathrm{i}\mu_1)\left(\exp[2\mu_1(x - 2\varsigma_1 z)] + \frac{1}{\mu_1}\right) - (\varsigma_2 + \mathrm{i}\mu_2)\left(\exp[2\mu_2(x - 2\varsigma_1 z)] + \frac{1}{\mu_2}\right)$$

and

$$g(x, z) = (\varsigma_1 - \mathrm{i}\mu_1)(\varsigma_2 - \mathrm{i}\mu_2)\left(\exp[2\mu_1(x - 2\varsigma_1 z)] + \frac{1}{\mu_1}\right) \times \left(\exp[2\mu_2(x - 2\varsigma_2 z)] + \frac{1}{\mu_2}\right) - \cdots - \frac{1}{(\mu_1 + \mu_2)^2}\left(\frac{1}{\varsigma_1 + \mathrm{i}\mu_1} + \frac{1}{\varsigma_2 + \mathrm{i}\mu_2}\right)^2,$$

with $\mu = \sqrt{1 - \varsigma_i^2}$. The two dark solitons involved in equation (3) are fully described by the parameters ς_i, which lie in the range $-1 < \varsigma_i < 1$ and determine the width of each soliton $1/\varsigma_i$, their contrast ς_i^2, and their transverse velocities $V = 2\varsigma_i$. If one of these ς_i is zero, the corresponding soliton will be a black soliton; otherwise, the soliton will be a gray soliton, with its width and contrast increasing and decreasing, respectively, as $|\varsigma_i|$ is increased.

As a representative example, in figure 1 we show the interaction of two ideal dark solitons, obtained by plotting equation (3) with $\varsigma_1 = 0.6$ and $\varsigma_2 = -0.4$. Note that the crossing of two dark solitons, in general, does not exhibit the oscillatory behaviour which characterizes the collision profile of bright solitons. As we will see later, this difference is of fundamental importance for the splitting capabilities of a crossing of two waveguides based on dark spatial solitons.

By setting $\varsigma_1 = \varsigma_2 = \varsigma$, equation (3) describes the interaction of two identical dark solitons travelling with opposite transverse velocities. As Z_0 controls the separation between the initial solitons, using large enough value of Z_0 in order to generate two well separated dark solitons, equation (3) can be used to properly analyse a symmetrical crossing of

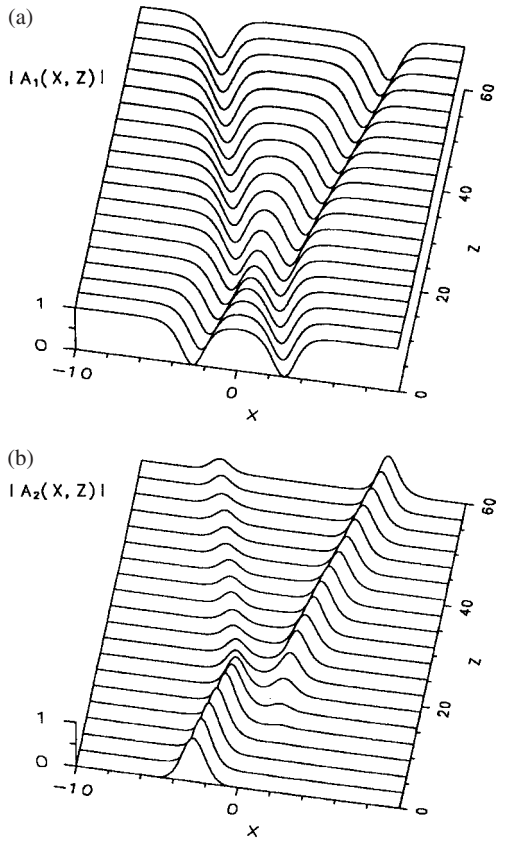

Figure 2. Optical Y junction based on ideal dark spatial solitons. (a) The waveguide crossing and (b) the trajectory followed by the probe beam. The parameters used were $\varsigma = 0.1$, $r_n = 1$, $Z_0 = 15$ and $\beta = 1.8$.

two dark spatial waveguides. Therefore, we use the following initial condition for the intense laser beam, A_1:

$$A_1(X, Z) \equiv \phi(X, Z_0) = 1 - \frac{4\exp(2vX)[\mathrm{i}\varsigma\sinh(4v\varsigma Z_0) - v\cosh(4v\varsigma Z_0)]}{1 - [\exp(4vX) + \frac{2}{v}\exp(2vX)\cosh(4v\varsigma Z_0) + \frac{1}{v^2}]}. \quad (4)$$

We stress here that the waveguide crossing generated by this initial condition is also ideal, in the sense that it still requires an infinite bright background. However, the practical realization of such a waveguide crossing can be performed if the appropriate two soliton solution of equation (4) is created on a wide enough laser beam. If this happens, we can launch a probe beam of a slightly different wavelength at one of the initial waveguides, and quantify the amount of its energy that can be split at the waveguide crossing. This probe beam can be coupled to the intense beam A_1 through the dynamic equation (2). As the initial condition for the probe beam we use

$$A_2(X, 0) = \exp(-(X - X_{20})^2/2\mu^2)\exp(\mathrm{i}V_{20}(X - X_{20})) \quad (5)$$

which represents a Gaussian beam centred at X_{20}, the initial position of the chosen optical channel (which depends on Z_0), and with transversal velocity V_{20} (which is determined by ζ). In figure 2 we have plotted a typical numerical simulation of (a) the waveguide crossing and (b) the trajectory of the probe

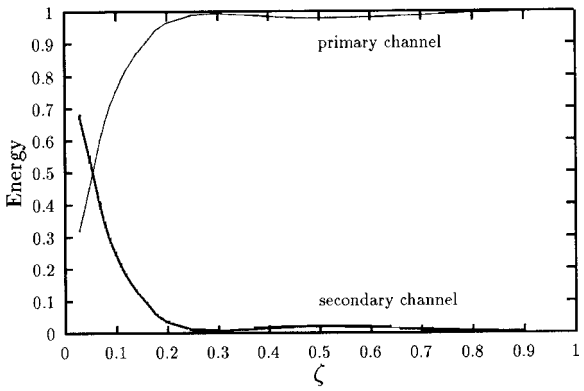

Figure 3. Relative probe beam energies after the crossing of two identical dark solitons as a function of the soliton parameter ς. The initial soliton-based waveguide is referred to as the primary optical channel. The fixed parameters were $r_n = 1$, $Z_0 = 15$ and $\beta = 1.8$.

beam, obtained by solving numerically equations (1) and (2) with the initial conditions given by equations (4) and (5), respectively, and using $\zeta = 0.1$, $\beta = 1.8$ (a nondegenerate wavelength case, $\lambda_1 \neq \lambda_2$) and $Z_0 = 15$. Figure 2(a) shows the waveguide crossing, which for this particular value of ζ, looks like as if the solitons do not cross each other. Instead, it appears that they repel each other as they approach the crossing region. On the other hand, figure 2(b) shows that the probe beam, initially launched to the left of the optical waveguide, is split at the crossing of the waveguides. Here, the original (primary) optical channel carries 75% of the initial probe beam energy after the crossing, while the secondary optical channel carries the remaining 25%.

The amount of probe beam energy that can be directed by the junction, as the soliton parameter ζ varies, is shown in figure 3. Here, it is shown that for large transversal velocities of the solitons (i.e. large values of ζ), almost all the probe beam remains at the primary optical channel, in agreement with previous theoretical work (Akhmediev and Ankiewicz 1993). However, as ζ decreases, the amount of the probe beam energy directed to the secondary optical channel monotonically increases, and it reaches significant values for $\zeta < 0.2$. This result is substantially different to the splitting properties of the bright soliton case where, for small collision angles, an oscillatory behaviour for the split energy was found. In addition to the monotonic behaviour of the energy split by the junction, shown in figure 3, the crossing of two ideal dark solitons has the severe inconvenience that the relative phase between the solitons cannot be varied. This is because they are not initially uncoupled as in the case of bright solitons. These two facts may restrict the photonics application of a collision of dark solitons to fixed splitters and interconnectors. However, it is important to give a physical reason for the differences found between the optical junctions based on bright and dark solitons.

3. Analysis

The numerical results found for the splitting of the probe beam energy shown in figure 3 can be explained as follows. As was found in a previous work (Torres-Cisneros *et al* 1993), the probe beam is diffracted at the soliton collision zone, therefore

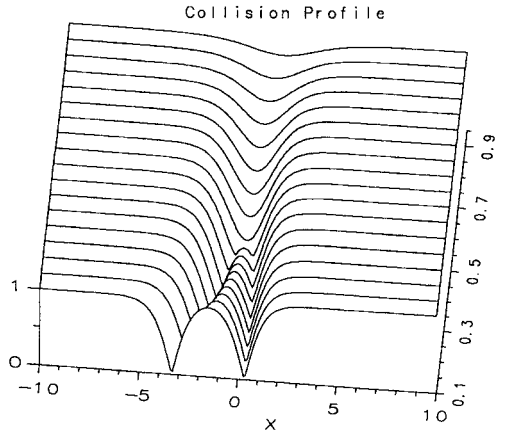

Figure 4. Profile of the collision pattern of two ideal dark solitons as a function of ζ. Note that for $\zeta < 1/2$, the collision profile possesses two dips.

the characteristics of the output probe beam basically depend on the diffractive screen. This diffractive screen, $T(X)$, is given by $T(X) = \exp(-\mathrm{i}h\beta\Psi(X))$, where h is its thickness and $\Psi(X)$ represents the intensity of the collision pattern. For the case of a collision of two identical dark solitons, the collision profile is taken from equation (4) with $Z_0 = 0$, that is:

$$\Psi(X) = |A_1(X,0)|^2 = \left|1 - \frac{4v^3\exp(2vX)}{(1-v^2)+v^2\exp(2vX)[\exp(2vX)+\frac{2}{v}]}\right|^2. \quad (6)$$

This profile is essentially different to that of the collision of two bright solitons. It does not exhibit an oscillatory behaviour and it depends on ζ (Torres-Cisneros *et al* 2003). This is shown in figure 4, where for small ζ it consist of two symmetrical dips of high contrast. As we increase the value of ζ, it causes the merging of those dips into a single one of low contrast. Therefore, the collision profile of two ideal dark solitons as a function of ζ has either one or two intensity dips.

The explanation of this dual behaviour is obtained by computing the minima of the collision profile. Equating to zero the X-derivative of $\Psi(X)$ in equation (6), we obtain that the left and right dips on the collision profile, labelled LD and RD, respectively, appear for $\zeta < 1/2$ and are centred at

$$X_{\mathrm{LD}} = \frac{1}{2v}\ln\left[\frac{1-2\varsigma^2}{v} - \sqrt{1-4\varsigma^2}\right],$$
$$X_{\mathrm{RD}} = \frac{1}{2v}\ln\left[\frac{1-2\varsigma^2}{v} + \sqrt{1-4\varsigma^2}\right], \quad (7)$$

while the central maximum for $\zeta < 1/2$ and minimum for $\zeta > 1/2$, labelled CD, is centred at

$$X_{\mathrm{CD}} = \frac{1}{4v}\ln\left[\frac{\varsigma^2}{v^2}\right]. \quad (8)$$

We note that the left and the right dips of the collision profile are not symmetrical about $X = 0$, and that their separation decreases as ζ approaches $1/2$ (figures 4 and 5). Physically, the two dips of $\Psi(X)$ appear because $A_1(X,0)$ has a single minimum at $X = X_{\mathrm{CD}}$, with $A_1(X_{\mathrm{CD}},0) = 2\varsigma - 1$. Therefore,

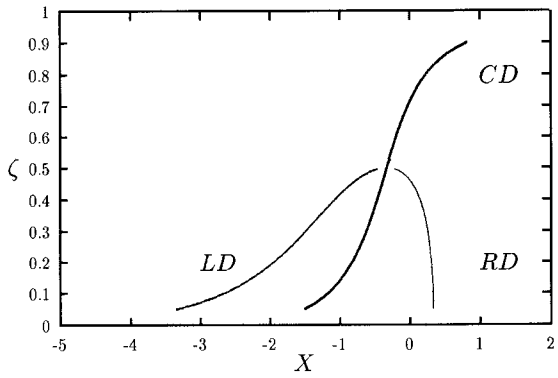

Figure 5. Position of the minima and the maximum of the collision profile of figure 4. LD and RD denote, respectively, the position of the left and right minima which appear for $\zeta < 1/2$. CD denotes the position of the central maximum for $\zeta < 1/2$ and the central minimum for $\zeta > 1/2$.

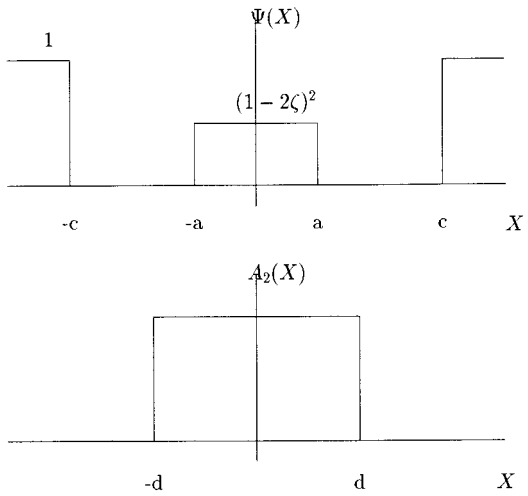

Figure 6. Approximated dark soliton collision and probe beam profiles for intermediate values of ζ.

$A_1(X_{\mathrm{CD}},0)$ is negative for $0 < \zeta < 1/2$ and its intensity profile, $\Psi(X)$, shows the two dips.

We have analysed the nature of $\Psi(X)$ in some detail because we anticipate that it will produce a complicated integral when we use it for computing the angular spectrum of the diffracted probe beam. Denoting by $A_{2\mathrm{d}} = T(X)A_2(X)$ the probe beam profile after the diffractive screen, where $A_2(X)$ is the initial probe beam at the collision point, its angular spectrum is given by

$$\tilde{A}_{2\mathrm{d}}(k_x) = \int A_2(X)\exp(-\mathrm{i}h\beta\Psi(X))\exp(-\mathrm{i}k_x X)\,\mathrm{d}X. \quad (9)$$

In order to obtain some insight into the main properties of $\tilde{A}_{2\mathrm{d}}$, we will use a simplified representation of $\Psi(X)$, instead of using a direct substitution of $\Psi(X)$ from equation (6). For example, for large collision angles, when $\zeta > 1/2$ and h is relatively small, we can use the approximation: $\Psi(X) \approx 1 - (\varsigma - 1)^2\sec h^2(X/v)$, which simulates the single dip structure of the collision pattern of figure 6. Under these conditions, the phase diffractive screen takes the form

$$\exp(-\mathrm{i}h\beta\Psi(X)) \approx 1 - \mathrm{i}h\beta\Psi(X) \approx 1 - \mathrm{i}h\beta[1-(\varsigma-1)^2\sec h^2(X/v)]. \quad (10)$$

Without introducing a significant additional approximation, we set $\tilde{A}_{2d}(X) = \sec h(X/v)\exp(iV_{20})$ (instead of equation (5) with $X_{20} = 0$), and obtain the angular spectrum of the diffracted probe beam:

$$\tilde{A}_{2d}(k_x) = \int \operatorname{sech}(X/v)[(1 - ih\beta) + ih\beta(\varsigma - 1)^2 \sec h^2(X/v)] \times \exp[-i(k_x - V_{20})X]\,dX$$

or

$$\tilde{A}_{2d}(k_x) = [(1 - ih\beta) + (ih\beta/2)(\varsigma - 1)^2(1 + (k_x - V_{20}^2))] \times \operatorname{sech}^2(\pi(k_x - V_{20})/2). \quad (11)$$

Note that the spectrum of the diffracted beam will be centred at the same frequency as that of the initial beam, and that its intensity, $1+h^2\beta^2[1+(\varsigma-1)^2/2]^2$, is not significatively affected by ζ when h is small. Therefore, for large collision angles there is basically no diffraction, and the probe beam is guided by the initial soliton-based waveguide after the soliton collision, as was numerically found in figure 3. On the other hand, when the collision angle is small; that is when ζ is close to zero, h is large and the phase of the diffractive screen oscillates rapidly. However, given the double dip structure of $\Psi(X)$ for $\zeta < 1/2$, we can use the method of stationary phase and, as a first approximation, consider that the main contribution to the integral of equation (9) comes from the point $X = X_{CD}$, where the collision profile has its central maximum (Jeffreys and Jeffreys 1978). In order to apply the method of stationary phase we take the second derivative of $\Psi(X)$ and evaluate it at X_{CD}. The result is: $\Psi''(X_{CD}) = -8v^4/(\varsigma + 1)^2$. Therefore, the spectral intensity of the diffracted probe beam at its initial central frequency, $k_x = V_{20}$, is estimated to be

$$|\tilde{A}_{2d}(V_{20})|^2 = \left|\int \operatorname{sech}(X - X_{CD})\exp(-ih\beta\Psi(X))\,dX\right|^2 \approx \frac{2\pi}{-h\beta\psi''(X_{CD})} \approx \frac{\pi\varsigma}{4\beta(1-\varsigma)^2}. \quad (12)$$

This equation establishes a monotonic decreasing of the intensity of the spectrum of the diffracted probe beam in the direction of the primary optical channel as ζ approaches zero, and it agrees with figure 2. It is important to note here that the same double dip profile of $\Psi(X)$ allows us to give an additional qualitative description of the splitting characterization of the waveguide crossing of figure 4, for intermediate values of ς ($\approx 1/2$), when neither equation (11) or (12) applies. This can be done by simplifying both the diffractive screen and the probe beam profiles to square-like functions, as is shown in figure 6. The key parameter in this approximation is the phase difference of the central region of the diffractive screen, $(1 - 2\varsigma)^2$. The ratio of the width of the central peak of the collision pattern, denoted by a, to the width of the probe beam, denoted by d, is also important because it determines the influence of the phase screen on the profile of the diffracted beam. For example, if $d < a$, all the information on the diffractive screen will be lost when we calculate the intensity of the diffracted beam. We can compute a in terms of ζ from equation (6) in a straightforward way, but the resulting lack of simplicity will shadow our basic idea[6]. Therefore, focusing on the physical description of this approximation, we assume $a < d < c$ to observe the influence of the approximated diffractive screen on the probe beam.

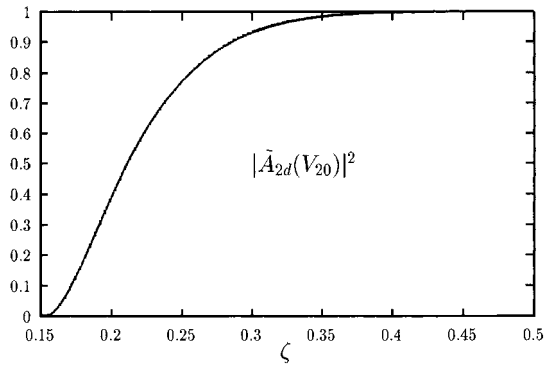

Figure 7. Intensity of the $k_x = V_{20}$ component of the diffracted probe beam as a function of ζ. Here, $h = 1/2\varsigma$ and $\beta = 2$.

Substitution of the particular profiles for $A_2(X)$ and $\Psi(X)$ of figure 6 into equation (9), followed by the respective integral gives

$$\tilde{A}_{2d}(k_x) = 2d\,\operatorname{sinc}[(k_x - V_{20})d] + 2a(\exp[-ih\beta(1 - 2\varsigma)^2] - 1)\operatorname{sinc}[(k_x - V_{20})a] \quad (13)$$

from which we can estimate the influence of varying ζ on the spectral distribution of the diffracted probe beam in the direction of the primary optical soliton-based waveguide. Setting $k_x = V_{20}$ in the equation above we obtain:

$$\tilde{A}_{2d}(k_x) = d^2\left[1 - 4\frac{a}{d}\left(1 - \frac{a}{d}\right)\sin^2[h\beta(1-2\varsigma)^2/2]\right]. \quad (14)$$

Figure 7 shows a graphical representation of this approximation. For the particular set of parameters used, $h = 1/2\varsigma$, $\beta = 2$, and $a/d = 1/2$, the curve obtained qualitatively describes the result of figure 3 for $0.15 < \zeta < 0.5$. For $\zeta < 0.15$, equation (14) predicts an oscillatory behaviour which is not present in figure 3, but it simply indicates that the approximation of equation (14) is no longer valid because of the rapid variations in the phase of the diffractive screen, and because the approximation based on the method of stationary phase of equation (12) has to be used instead.

4. Conclusions

The three approximations we have presented, for large, small and intermediate values of ζ, allows us to conclude that the basic physical mechanism behind the splitting of a junction based on ideal dark solitons is also diffraction. Thus, though the corresponding phase diffractive screen possesses quite a different structure in the bright and dark soliton cases, the physics involved is the same. This is a very important result, that unifies the theoretical description of the behaviour followed by a weak probe beam during the crossing of two optical waveguides, bright or dark, in Kerr type media.

[6] The width of the central peak of the collision pattern is given by: $a = X_m - X_{CD}$ where $X_m = (1/2v)\ln\{(1 + 2\zeta)/v \pm [(3\zeta + 1)/(1 - \zeta)]^{1/2}\}$.

References

Agrawal G P 2002 *Nonlinear Fiber Optics* 3rd edn (San Diego, CA: Academic) chapter 7

Akhmediev N and Ankiewicz A 1993 *Opt. Commun.* **100** 186

Blow K J and Doran N J 1985 Multiple dark soliton solutions of the nonlinear Schroedinger equation *Phys. Lett.* A **107** 55

De la Fuente R, Barthelemy A and Froehely C 1991 Spatial-soliton induced guided waves in a homogeneous nonlinear Kerr medium *Opt. Lett.* **16** 793

Islam M N, Soccolich C C E and Gordon J P 1992 Ultrafast digital soliton logic gates *Opt. Quantum Electron.* **24** 1215

Jeffreys H and Jeffreys B S 1978 *Methods of Mathematical Physics* (London: Cambridge University Press) chapter 17

Kodama Y and Hasegawa A 1991 Effects of the initial overlap on the propagation of optical solitons at different wavelengths *Opt. Lett.* **16** 208

Luther-Davies B and Xiaoping Y 1992 Waveguides and Y junctions formed in bulk media by using dark spatial solitons *Opt. Lett.* **17** 496

Shalaby M and Barthelemy A 1992 Ultrafast photonic switching and splitting through cross phase modulation with spatial solitons couple *Opt. Commun.* **94** 341

Thurston R N and Weiner A M 1991 Collisions of dark solitons in optical fibers *J. Opt. Soc. Am.* B **8** 471

Tomlinson W J and Hawkings R J 1989 Dark solitons with finite-width background pulses *J. Opt. Soc. Am.* B **6** 329

Torres-Cisneros G E, Romero-Troncoso R J, Sanchez-Mondragon J J and Alvarado-Mendez E 1995 Collision of to real dark spatial solitons *J. Mod. Opt.* **42** 2323

Torres-Cisneros G E, Sanchez-Mondragon J J and Vysloukh V A 1993 Asymmetric optical Y junctions and switching of weak beams using bright spatial soliton collisions *Opt. Lett.* **18** 1299

Torres-Cisneros M, Meneses-Nava M A, Haus J W, Aguilera-Cortés L A, Guzman-Cabrera R, Sanchez-Mondragón J and Trejo M 2003 Mechanisms of crossing for two optical waveguides based on dark spatial solitons *Acta Universitaria* **13** 3

Zhao W and Bourkoff E 1989 Interactions between dark solitons *Opt. Lett.* **14** 1371